U.S. National Library of Medicine
National Center for Biotechnology Information

NLM Citation: Chopra A. ^{125}I-Labeled single-chain monoclonal antibody, NS4F5, that targets the GlcNS6S-IdoA2S motif of heparan sulfate proteoglycans for the *in vivo* imaging of peripheral amyloidosis. 2011 Nov 4 [Updated 2011 Dec 1]. In: Molecular Imaging and Contrast Agent Database (MICAD) [Internet]. Bethesda (MD): National Center for Biotechnology Information (US); 2004-2013.
Bookshelf URL: https://www.ncbi.nlm.nih.gov/books/

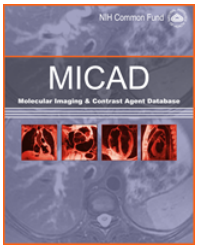

^{125}I-Labeled single-chain monoclonal antibody, NS4F5, that targets the GlcNS6S-IdoA2S motif of heparan sulfate proteoglycans for the *in vivo* imaging of peripheral amyloidosis

[^{125}I]-NS4F5

Arvind Chopra, PhD[1]

Created: November 4, 2011; Updated: December 1, 2011.

Chemical name:	^{125}I-Labeled single-chain monoclonal antibody, NS4F5, that targets the GlcNS6S-IdoA2S motif of heparan sulfate proteoglycans for the *in vivo* imaging of peripheral amyloidosis	
Abbreviated name:	[^{125}I]-NS4F5	
Synonym:		
Agent Category:	Antibody	
Target:	GlcNS6S-IdoA2S motif of heparan sulfate proteoglycans	
Target Category:	Antigen	
Method of detection:	Single-photon emission computed tomography (SPECT); gamma planer imaging	
Source of signal / contrast:	^{125}I	
Activation:	No	
Studies:	• *In vitro* • Rodents	Structure not available in PubChem.

Background

[PubMed]

Peripheral amyloidosis is the extracellular deposition of insoluble protein fibrils in various organs of animals, including humans, and these deposits are considered to be biomarkers for diseases such as Alzheimer's disease (AD), light chain amyloidosis (AL), etc (1). The fibrils are made up of disease-specific aggregated proteins or peptides (e.g., Aβ peptides for AD, light chains for AL or multiple myeloma, and reactive amyloidosis (AA)) that incorporate heparin sulfate proteoglycans (HSPG; heparin belongs to the heparan sulfate family of proteoglycans that contain the $(GlcNS6S\text{-}IdoA2S)_3$ motif)) and the serum amyloid P component (SAP) within their structure during disease progression. A characteristic feature of the protein fibrils is that the constituent

Author Affiliation: 1 National Center for Biotechnology Information, NLM, Bethesda, MD 20894; Email: micad@ncbi.nlm.nih.gov.

proteins form a secondary cross-β pleated sheet structure that is resistant to proteolytic digestion (for structural details, see Goldsbury et al. (2)). In addition, clinical symptoms of amyloidosis in a patient are influenced by the degree to which an organ is involved in the disease (3).The HSPG contain diverse types of oligosaccharides that are sulfated on the hydroxyl moieties to varying degrees, and these hypersulfated structures are distinct, are found specifically in the amyloid deposits, and differ from one another depending on the organ where they are located (4). In addition, the HSPG contain stretches of the disaccharide GlcNS6S-IdoA2S (HS^{NS4F5}; these motifs are abundantly found in heparin, but have limited presence in the HS of normal tissues) that inhibit cell proliferation and induce apoptosis but do not affect the attachment of cells to collagen I (5). Because the HSPG in the amyloids are hypersulfated compared to the proteoglycans in normal tissues, HSPG are considered to be suitable for the detection of amyloids with imaging techniques and to diagnose and monitor amyloidosis progression and to determine the prognosis for a patient with amyloidosis (1).

Whole-body scintigraphy with radioiodinated SAP is commonly used in Europe for the detection of amyloidosis in the various parts of the body, but this technique is not approved by the United States Food and Drug Administration for clinical use in United States because the SAP used to generate the tracer is isolated from human sources (1). In an attempt to develop an amyloid imaging agent that would not require the use of human materials, Wall et al. showed that a ^{125}I-labeled synthetic heparin-binding peptide, p5, could be used with single-photon emission computed tomography (SPECT) to detect amyloid deposits in H2/huIL-6 transgenic mice with severe systemic AA amyloidosis (AA mice) (1). In another study, Wall et al. evaluated the use of ^{125}I-labeled single chain (scFv) antibodies (Abs) directed against HS for the detection of amyloids in AA mice that are prone to develop amyloidosis at ~4–5 months of age as described elsewhere (6). Among these radioiodinated scFv Abs, NS4F5, which binds specifically to HS^{NS4F5} (5), has been determined to be the most suitable for the noninvasive imaging of amyloids in the transgenic animals (6).

Related Resource Links

Related chapters in MICAD

Clinical trials related to amyloidosis

Amyloidosis in Online Mendelian Inheritance in Man Database (OMIM)

Protein sequence of human amyloid

Crystal structures of human amyloid proteins

Symptoms, diagnosis, and treatment of amyloidosis (at Cedars-Sinai Medical Center, LA)

Synthesis

[PubMed]

Anti-HS scFv Abs (HS4C3, NS4F5, HS4E4, and the chondroitin sulfate–binding scFv Ab GD3G7) were produced and purified as described by Wall et al. (6). The antibodies were labeled with ^{125}I using the chloramine-T method and the labeled Abs were purified with gel filtration on Sepharose Aca 44 gel in 0.01 M sodium phosphate (pH 7.6) and 0.15 M sodium chloride containing 5 mg/mL bovine serum albumin. The radiochemical purity (RCP) of the labeled Abs was evaluated with SDS/PAGE and phosphorimaging (6). The radiochemical yield, RCP, and specific activity of the labeled Abs were 50.9 ± 10.0%, 96.6 ± 2.8%, and 25–40 μCi/nmol protein, respectively.

In Vitro Studies: Testing in Cells and Tissues

[PubMed]

The binding specificities of the various Abs to the chemical groups in HS (for HS4C3, NS4F5, and HS4E4) and chondroitin sulfate (for GD3G7) were established with the ELISA technique and have been described by Wall et al. (6).

Animal Studies

Rodents

[PubMed]

The biodistribution of the ^{125}I-labeled Ab fragments (scFv) was investigated in amyloidosis induced in AA mice as described by Wall et al. (6). The amyloid deposits were found primarily in the liver, spleen, and pancreas of these animals. Wild-type (WT) mice from the same colony (identified by genotyping; non-transgenic) were used as controls for this study. The animals (n = 3 animals/Ab) were injected with ~7.40 MBq (~200 μCi; ~25 μg) of the labeled Abs through the lateral tail vein and euthanized 1–4 h later by isoflurane inhalation overdose. SPECT/Computed tomography (CT) images of the animals were subsequently acquired, and all major tissues were collected for biodistribution measurement (data were expressed as percent of injected dose per gram tissue (% ID/g)) and microautoradiography. At 1 h postinjection (p.i.), no difference in the uptake of radioactivity in the various organs of the AA and the WT mice was apparent with any Ab. However, because the AA mice are known to have slow clearance of ScFv Abs through the kidneys due to the amyloid pathology, the tissue/muscle (T/M) ratios were calculated from the data. Among the different Abs, only NS4F5 showed at least a two-fold higher T/M ratio in the liver, spleen, and kidneys of AA mice compared to the same organs from the WT animals. No other labeled Ab showed a similar increase in the ratio except HS4E4, which had a more than two-fold T/M ratio in the kidneys of the AA mice compared to the WT animals. In general, the kidneys (9%–13% ID/g) and the stomach (11%–22% ID/g) of the WT mice showed the highest concentration of radioactivity, and the investigators attributed this to renal catabolism and dehalogination of the radioiodinated Ab followed by sequestering of the ^{125}I iodide to the stomach (this organ has a high concentration of iodide symporters). At 4 h p.i., most of the radioactivity from the Abs was associated with the liver and kidneys in the AA mice (these organs have large amounts of amyloid deposits), and this was confirmed with SDS/PAGE analysis of the various tissues of animals treated with ^{125}I-NS4F5 (the labeled scFv chains ran midway on the gel, whereas the ^{125}I iodide ran just ahead of the dye front; the *Rf* values for the two fractions were not reported). A similar analysis of tissues obtained from the WT mice showed that the radioactivity was present largely as free radioiodide except in the kidney, which had some label bound to the scFv.

For SPECT/CT imaging, the AA and WT mice (n = 3 animals/Ab) were injected with the radioiodinated scFvs as described above, and the images were acquired while the rodents were under anesthesia (6). At 1 h p.i., images of the WT mice injected with the different Abs showed that radioactivity was present mainly in the stomach while trace amounts of the label were detected in the kidneys. In addition, from the images it was evident that only ^{125}I-NS4F5 had a distinct distribution in the AA mice because the liver and spleen of these animals showed a higher uptake of radioactivity compared to the organs of the WT animals. This indicated that the scFv NS4F5 was probably the most suitable for the imaging of amyloid deposits in the mice. No blocking studies were reported.

To confirm that ^{125}I-NS4F5 was indeed the most suitable scFv Ab for the imaging of amyloid deposits, a second biodistribution and SPECT/CT imaging study was performed with this tracer (6). The AA and WT mice (n = 3 mice/group/time point) were injected with 4.5 MBq (120 μCi) ^{125}I-NS4F5, and SPECT/CT images were acquired from the animals under anesthesia at 1, 4, and 24 h p.i. Images acquired at 1 h p.i. showed that the radioactivity was present mainly in the liver and spleen of the AA mice, whereas in the WT mice the label was observed primarily in the stomach and the thyroid. At 4 h p.i., the images of the AA and the WT mice looked similar, thus indicating that the labeled scFv was lost from the amyloid deposits in the AA mice and the WT

animals at this time point. At 1 h p.i. the thyroid of the WT and the AA animals showed a similar accumulation of the label, but at 4 h p.i the amount of radioactivity in the AA thyroid was ~5 fold (~2%ID/g) that of the WT mice. From this observation, the investigators concluded that 1 h p.i. was the best time point to image the amyloid deposits in these animals. By 24 h p.i., little radioactivity remained in the animals (AA and WT) to acquire any images (6). Biodistribution measurements of the different tissues at 1, 4, and 24 h confirmed the SPECT/CT imaging data. At 1 h p.i., the AA mice had more than two-fold higher radioactivity in the liver, spleen, and kidneys compared to the same organs from the WT animals. By 4 h p.i., this difference increased to approximately four-fold, and by 24 h p.i., although most of the label had cleared from the organs of the AA and the WT mice, the AA/WT ratio for most organs were similar but remained >1. The investigators suggested that this was probably due to a defective renal function, which leads to slow clearance of the label from the AA animals.

On the basis of results obtained from the studies described above, the investigators concluded that scFv NS4F5 requires further improvement before it can be used as an agent for imaging amyloid deposits (6).

Other Non-Primate Mammals

[PubMed]

No publication is currently available.

Non-Human Primates

[PubMed]

No publication is currently available.

Human Studies

[PubMed]

No publication is currently available.

Supplemental Information

[Disclaimers]

No information is currently available.

NIH Support

Studies reported in this chapter were supported by National Institute of Diabetes and Digestive and Kidney Diseases Award R01DK079984.

References

1. Wall J.S., Richey T., Stuckey A., Donnell R., Macy S., Martin E.B., Williams A., Higuchi K., Kennel S.J. *In vivo molecular imaging of peripheral amyloidosis using heparin-binding peptides.* . Proc Natl Acad Sci U S A. 2011;108(34):E586–94. PubMed PMID: 21807994.
2. Goldsbury C., Baxa U., Simon M.N., Steven A.C., Engel A., Wall J.S., Aebi U., Muller S.A. *Amyloid structure and assembly: insights from scanning transmission electron microscopy.* . J Struct Biol. 2011;173(1):1–13. PubMed PMID: 20868754.
3. Perfetto F., Moggi-Pignone A., Livi R., Tempestini A., Bergesio F., Matucci-Cerinic M. *Systemic amyloidosis: a challenge for the rheumatologist.* . Nat Rev Rheumatol. 2010;6(7):417–29. PubMed PMID: 20531382.

4. Ori A., Wilkinson M.C., Fernig D.G. *The heparanome and regulation of cell function: structures, functions and challenges.* . Front Biosci. 2008;13:4309–38. PubMed PMID: 18508513.
5. Smits N.C., Kurup S., Rops A.L., ten Dam G.B., Massuger L.F., Hafmans T., Turnbull J.E., Spillmann D., Li J.P., Kennel S.J., Wall J.S., Shworak N.W., Dekhuijzen P.N., van der Vlag J., van Kuppevelt T.H. *The heparan sulfate motif (GlcNS6S-IdoA2S)3, common in heparin, has a strict topography and is involved in cell behavior and disease.* . J Biol Chem. 2010;285(52):41143–51. PubMed PMID: 20837479.
6. Wall, J.S., T. Richey, A. Stuckey, R. Donnell, A. Oosterhof, T.H. van Kuppevelt, N.C. Smits, and S.J. Kennel, *SPECT imaging of peripheral amyloid in mice by targeting hyper-sulfated heparan sulfate proteoglycans with specific scFv antibodies.* Nucl Med Biol, 2011